



ELSEVIER

Polymer 43 (2002) 6561–6568

polymerwww.elsevier.com/locate/polymer

Hydrogen bonding and polyurethane morphology. II. Spectroscopic, thermal and crystallization behavior of polyether blends with 1,3-dimethylurea and a model urethane compound

Emel Yilgör, Ersin Yurtsever, Iskender Yilgör*

Department of Chemistry, Koç University, Rumelifeneri yolu, Sariyer 80910, Istanbul, Turkey

Received 3 April 2002; received in revised form 3 July 2002; accepted 19 August 2002

Abstract

Thermal, structural and spectroscopic behavior of the blends of poly(ethylene oxide)glycol (PEO) with a model urethane compound bis(4-butylcarbamato-cyclohexyl)methane and 1,3-dimethylurea (DMU) were investigated by differential scanning calorimetry (DSC) and hot-stage optical microscopy (HOM). Blends with a wide range of compositions were prepared in tetrahydrofuran (THF) solutions and dried. DSC results indicated the formation of two-phase structures consisting of a pure polyether phase and a highly mixed DMU–polyether phase. As the amount of polyether in the blends was increased, the melting endotherm of DMU became much broader and shifted to lower temperatures, indicating extensive mixing with PEO. The mixed phase was also crystalline. This was strongly supported by HOM results. While pure PEO and DMU crystals showed spherulitic structures, mixed DMU–PEO phase showed fibrillar crystals. Consecutive heating–cooling cycles of the blends did not result in any changes in the blend morphologies. Formation of strong hydrogen bonding between DMU and PEO was also demonstrated by FTIR spectroscopy from the shifts in (N–H and C=O) absorption peaks. © 2002 Published by Elsevier Science Ltd.

Keywords: Polyurethane; Hydrogen bonding; Morphology

1. Introduction

Segmented polyurethanes (PU) and polyurethaneureas (PUU) constitute one of the most interesting classes of synthetic elastomers. Due to the availability of very large number of starting materials, it is possible to prepare PU and PUU type copolymers with properties ranging from soft rubbery materials to tough engineering polymers [1–3]. It is well documented that the properties and performance of segmented PU and PUU copolymers are strongly dependent on their microphase morphologies [1–5]. It has also been demonstrated that, depending on their backbone structures and compositions, these copolymers exhibit two phase morphologies, which usually consist of a continuous, soft rubbery matrix in which hard segment domains are distributed [1–7]. It is generally accepted that a major factor for the phase separation is the strong hydrogen

bonding between urethane and urea type hard segments [8–12] and/or hard segment crystallization [10,13].

Our investigations on the preparation, characterization and properties of model segmented polyurethanes and polyureas based on polydimethylsiloxane (PDMS) and polyether soft segments displayed some very unexpected results [14,15]. When the mechanical properties of polyurea copolymers prepared from amine terminated PDMS and PEO oligomers are compared, it was very surprising to note that although PDMS based systems showed excellent mechanical properties, PEO based systems had almost no mechanical strength at all. Stress–strain behavior of two homologous polyurea copolymers, prepared by the stoichiometric reaction of bis(4,4'-isocyanatocyclohexyl)methane (HMDI) and amine terminated $M_n = 800$ g/mol PEO and $M_n = 800$ g/mol PDMS oligomers is provided in Fig. 1. Both of these materials have exactly the same hard and soft segment contents of 24.7 and 75.3 wt%, respectively. As can be seen in Fig. 1, the siloxane–urea copolymer (PSU) shows fairly high modulus (125 MPa) and tensile strength (17.8 MPa) values and 550% elongation at break.

* Corresponding author.

E-mail address: iyilgor@ku.edu.tr (I. Yilgör).

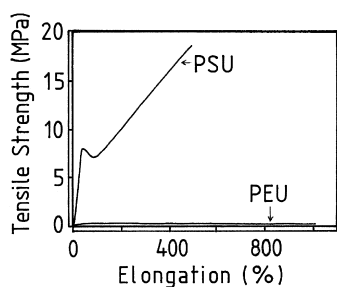


Fig. 1. Stress–strain curves for polysiloxane–urea (PSU) and polyether–urea (PEU) copolymers with similar backbone structures.

On the other hand, the polyether–urea copolymer (PEU) is extremely weak and shows a tensile strength value of less than 0.25 MPa. We believe substantial differences between the tensile behavior of these two systems are mainly due to excellent phase separation in PDMS based system [16] and extensive phase mixing in the PEO based system, which is due to strong the hydrogen bonding between urea hard segments and polyether soft segments [9,17].

As explained in Ref. [18], in order to understand the strength (and extent) of the competitive hydrogen bonding between urethane/ether and urea/ether groups, advanced quantum mechanical (QM) calculations based on density functional theory (DFT) were performed. From DFT calculations, hydrogen bond energies between urea–urea and urea–ether were calculated to be 58.5 and 29.4 kJ/mol and between urethane–urethane and urethane–ether were calculated to be 46.5 and 23.6 kJ/mol, respectively. On the other hand, hydrogen bond energy between ureas and siloxane was only 7.5 kJ/mol [14]. These results clearly indicate the possibility of extensive phase mixing between urethane/ether and urea/ether groups due to strong hydrogen bonding. They also strongly support the stress–strain behavior of siloxane–urea and polyether–urea segmented copolymers, in Fig. 1.

Strong support to the results obtained in QM calculations is provided by the investigations of Coleman and co-workers, who have experimentally demonstrated that a model amorphous polyurethane and an amorphous polyether, based on ethylene oxide and propylene oxide units were completely miscible in every composition [19]. All these results, together with those reported by others [20–23], clearly indicate that, the dominating factor for the phase separation in segmented polyurethanes and polyureas may be the crystallization of the hard segments. If the hard segments were amorphous, it would be very difficult to observe phase separation in polyether or polyester based PU or PUU copolymers. This would only lead to the formation of materials with poor mechanical properties [1,24].

In order to experimentally confirm the results of QM calculations [18] and better understand the influence of competitive hydrogen bonding between hard and soft segments on the phase behavior of urethane/ether and urea/ether systems, model blends of PEO with 1,3-

dimethylurea (DMU) and bis(4-butylcarbamato-cyclohexyl)-methane (URTN) were investigated. Thermal, spectroscopic and morphological behavior of blends prepared in a wide composition range were studied by differential scanning calorimetry, FTIR spectroscopy and hot stage optical microscopy.

2. Experimental

2.1. Materials

Reagent grade urea (U), 1,3-dimethylurea (DMU) and 1,1,3,3-tetramethylurea (TMU) were obtained from Aldrich and were used as received. Poly(ethylene oxide)glycol (PEG) ($M_n = 1500$ g/mol) was obtained from Union Carbide. α,ω -aminopropyl terminated polydimethylsiloxane oligomer (PDMS) ($M_n = 900$ g/mol) was obtained from Th. Goldschmidt AG, Essen, Germany. α,ω -Propylamine terminated poly(ethylene oxide) oligomer (PEO) ($M_n = 900$ g/mol) was obtained from Huntsman Corporation. Bis(4-isocyanatocyclohexyl)methane (HMDI) with a purity of greater than 99.5% was supplied by Bayer AG. Spectroscopic grade tetrahydrofuran (THF) was obtained from Riedel-de-Haen.

2.2. Synthetic methods and preparation of blends

Synthesis and structural characterization of bis(4-butylcarbamato-cyclohexyl)methane (URTN) has already been reported [14]. Siloxane–urea and polyether–urea copolymers were prepared in three neck round bottom flasks fitted with an overhead stirrer, nitrogen inlet and an addition funnel. Calculated amounts of HMDI were introduced into the flask and dissolved in THF. Stoichiometric amounts of PDMS (or PEG) oligomers were separately dissolved in DMF in an Erlenmeyer flask and introduced into the addition funnel. Reactions were conducted at room temperature by the drop-wise addition of HMDI solution into the reaction flask. Completion of the reactions were followed by monitoring the disappearance of strong isocyanate peak at 2260 cm^{-1} using FTIR spectroscopy.

PEO/DMU and PEO/URTN blends were prepared in Pyrex vials with a screw top. Desired amounts of each ingredient (to make a total weight of about 1.0 g) were weighed into the vial and dissolved in 5 ml of THF. All blends yielded clear solutions. THF was then evaporated, first at room temperature and then in a vacuum oven at 35°C . Blends were kept in a desiccator until further characterization. Blend compositions are given in wt/wt.

2.3. Characterization methods

Spectroscopic characterization of the products was obtained on a Nicolet Impact 400D FTIR spectrometer, with a resolution of 2 cm^{-1} . In these studies, thin blend

films were cast on KBr disks from THF solutions and dried in vacuum oven. DSC analyses of the products were obtained on a Rheometrics PL-DSC Plus instrument, under nitrogen atmosphere with a heating rate of 5 °C/min. Temperature and enthalpy calibration of DSC were obtained by using indium, lead and tin standards. Optical micrographs of the blends were obtained by using a Leica optical microscope fitted with a polarizer, hot stage and a CCD camera. Heating rate of the hot stage on the microscope was 1 °C/min. While taking photographs, temperature of the hot stage was kept constant.

3. Results and discussion

Segmented polyurethanes and polyurethaneureas are probably the most widely investigated copolymer systems both by academic and industrial researchers. It has been demonstrated that interesting solid-state properties of segmented polyurethanes and polyureas are due to the phase separation between hard (urethane, urea) and soft (polyether, polyester, polysiloxane) segments. Microphase morphologies of elastomeric systems consist of a continuous soft segment interconnected with hard segment domains. Although there is a general agreement on the two-phase morphologies of polyurethanes, there is limited information on the extent of molecular interactions between hard and soft segments and the actual composition (or purity) of the hard and soft segment phases. It has been demonstrated that when hard and soft segments are not inherently soluble in each other, or do not form any hydrogen bonding, such as siloxane–urea copolymers, they display well-separated microphase morphologies and excellent thermal and mechanical properties, which is a linear function of the amount of urea groups present in the system [14].

When the free energy of mixing ($\Delta G_{\text{mix}} = \Delta H_{\text{mix}} - T\Delta S_{\text{mix}}$) is considered, two factors seem to have the most important contribution for polyurethanes at room temperature, which are highly exothermic and included in the enthalpy (ΔH_{mix}) term. These are (i) the competitive hydrogen bonding between hard–hard and hard–soft segments and their H-bond energies, which are $\Delta H_{\text{hb-hh}}$ and $\Delta H_{\text{hb-hs}}$ indicating H-bond energies between hard–hard and hard–soft segments, respectively, and (ii) crystallization of pure hard and soft segments and as described later, formation of a new mixed crystalline phase and their enthalpies of fusion ($\Delta H_{\text{fus-hard}}$), ($\Delta H_{\text{fus-soft}}$) and ($\Delta H_{\text{fus-mixed}}$). When the influence of hydrogen bonding and crystallization on the entropy term is considered, both will result in the reduction of the entropy. In Ref. [18], we have already demonstrated by QM calculations that extensive hydrogen bonding interaction exists between ether oxygen and urea and urethane groups, with H-bond energies in the range of 23–30 kJ/mol [18]. The influence of hydrogen bonding on the melting points and enthalpy of fusion values of urea and substituted ureas are given in Table 1. As

Table 1

Melting points and enthalpy of fusion values for urea compounds determined by DSC

Compound	Code	T_m (°C)	ΔH_{fus} (J/g)
Urea	U	138	215.8
1,3-Dimethylurea	DMU	108	123.8
1,1,3,3-Tetramethylurea	TMU	–3	83.7

expected, there is a substantial difference between the melting points (T_m) of hydrogen bonded compounds (U and DMU) and TMU, which cannot form hydrogen bonds internally in pure form. Similar behavior is observed in the heat of fusion values of these compounds. Urea, with four hydrogens capable of forming hydrogen bonds, has a fairly high ΔH_{fus} value of 215.8 J/g. DMU, with only two hydrogens, has a ΔH_{fus} value of 123.8 J/g. TMU, with no capacity of internal hydrogen bonding has a ΔH_{fus} value of 83.7 J/g.

As a follow-up to our QM calculations, which suggests extensive competitive hydrogen bonding between ether and urea or urethane groups, we investigated the behavior of model systems experimentally. Poly(ethylene oxide)glycol (PEO) oligomer ($M_n = 1500$ g/mol) was used as the model ether, bis(4-butylcarbamato)cyclohexylmethane (URTN) and 1,3-dimethylurea (DMU) were used as model urethane and urea, respectively.

3.1. FTIR investigation

IR spectroscopy is a convenient technique for the semi-quantitative determination of the extent and strength of hydrogen bonding in organic molecules and polymers [9,10,25–27]. The principle is based on the shifts observed in the IR peaks for groups such as (N–H) and (C=O) due to hydrogen bond formation. IR spectra of PEO-1500 and DMU are provided in Fig. 2, together with a 50/50 blend as

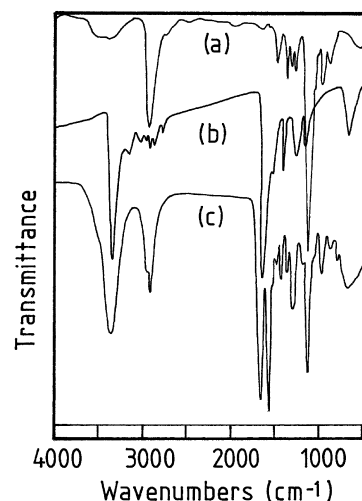


Fig. 2. FTIR spectra of (a) poly(ethylene oxide)glycol (PEO); (b) 1,3-dimethylurea (DMU) and (c) 50/50 by weight blend of PEO/DMU.

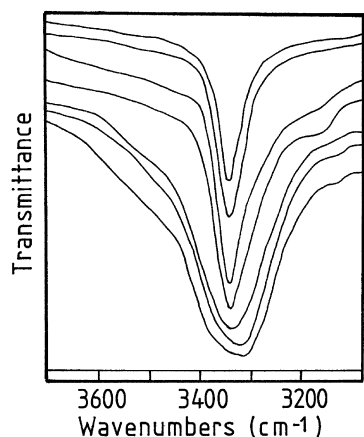


Fig. 3. N–H region in the FTIR spectra for DMU and PEO/DMU blends with different compositions. From top to bottom: pure DMU, 10/90, 25/75, 33/67, 50/50, 75/25 and 90/10 PEO/DMU by weight.

reference. As expected, PEO shows a very broad (O–H) peak between 3500 and 3300 cm^{-1} and a very sharp (C–O–C) stretching peak at 1107 cm^{-1} . DMU has very sharp and symmetrical (N–H) and (C=O) peaks at 3342 and 1624 cm^{-1} , respectively. On the other hand 50/50 blend shows a strong, broad peak at 3333 cm^{-1} , a sharp doublet at 1651 and 1569 cm^{-1} and a sharp ether peak at 1107 cm^{-1} . Fig. 3 shows the (N–H) region in the FTIR spectra of PEO/DMU blends with different compositions. In pure DMU peak minimum for (N–H) absorption is at 3342 cm^{-1} . As the amount of PEO in the blend is increased, the peak minima gradually shift to lower wavenumbers, reaching to a value of 3315 cm^{-1} for a blend composed of 90/10 wt/wt of PEO/DMU. These results indicate extensive hydrogen bonding between urea (N–H) hydrogens and the ether

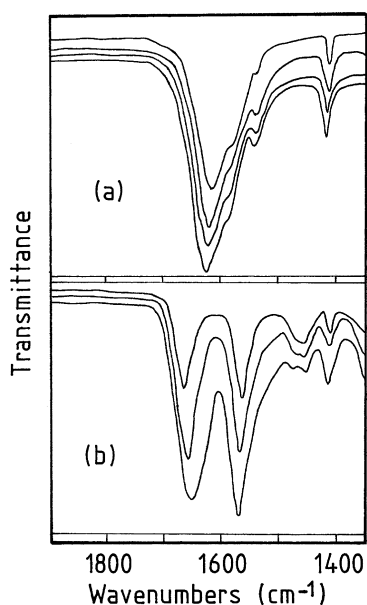


Fig. 4. FTIR spectra of the carbonyl region for pure DMU and PEO/DMU blends. From top to bottom: (a) 33/67, 25/75, 10/90 PEO/DMU by weight and pure DMU; (b) 90/10, 75/25 and 50/50 PEO/DMU by weight.

Table 2

FTIR peak positions and peak shifts due to hydrogen bonding for PEO/DMU blends

Sample description	N–H (cm^{-1})	Shift (cm^{-1})	C=O (cm^{-1})	Shift (cm^{-1})
DMU	3342	–	1624	–
PEO/DMU (10/90)	3341	1	1624	–
PEO/DMU (25/75)	3339	3	1626	2
PEO/DMU (33/67)	3335	7	1628	4
PEO/DMU (50/50)	3333	9	1651	27
PEO/DMU (75/25)	3321	21	1660	36
PEO/DMU (90/10)	3315	27	1667	43

oxygen. The carbonyl region in the FTIR spectra for the blends are shown in Fig. 4a and b. Fig. 4a gives the FTIR spectra of pure DMU and blends containing higher than 50 wt% DMU. All these blends have strong C=O absorption peaks with minima between 1624 and 1628 cm^{-1} , which also has a shoulder (amide II band) at 1586 cm^{-1} . On the other hand, as shown in Fig. 4b, blends containing 50 wt% or less amount of DMU show two well resolved peaks, one due to C=O (1653–1667 cm^{-1}) and the other due to amide II (1565–1569 cm^{-1}). C=O peaks show substantial increase to higher wavenumbers as the amount of PEO in the system is increased. These results (as also predicted by quantum calculations) clearly demonstrate that, as more PEO is added into the system, due to strong competition, hydrogen bonding between N–H and C–O–C increases at the expense of the hydrogen bonding between N–H and C=O, which is reflected by a shift in C=O peak position to higher wavenumbers. No shift in the ether peak at 1107 cm^{-1} is observed. The analyses of FTIR spectra and peak positions are summarized in Table 2.

3.2. DSC studies

Fig. 5 gives the DSC thermograms of starting materials, PEO, DMU and the model urethane (URTN). All starting material give fairly symmetrical and sharp melting endotherms, as expected for pure compounds. Melting point (T_m) for DMU and PEO obtained from these endotherms are 108 and 49 $^{\circ}\text{C}$, respectively, which are in

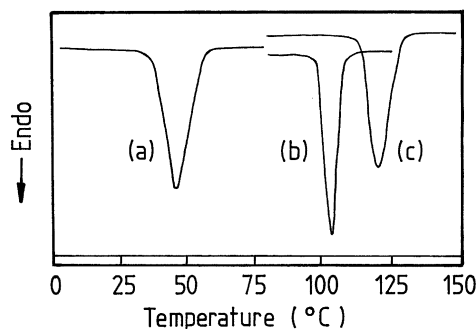


Fig. 5. DSC melting endotherms for (a) PEO; (b) DMU and (c) model urethane compound (URTN).

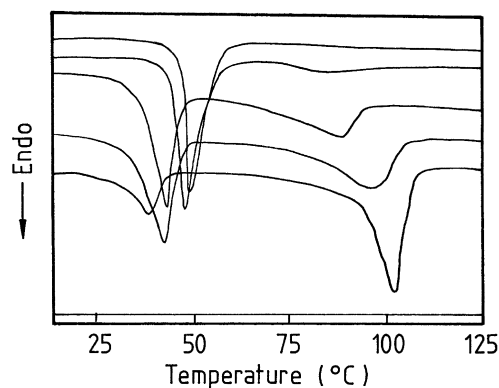


Fig. 6. DSC thermograms for PEO/DMU blends. From top to bottom: 90/10, 75/25, 50/50, 33/67 and 25/75 PEO/DMU by weight.

very good agreement with the literature values [28,29]. Melting point of URTN is 120 °C. Enthalpy of fusion (ΔH_{fus}) values obtained from the area under these endotherms for PEO, DMU and URTN are 150.5, 123.3 and 79.0 J/g, respectively.

DSC thermograms for PEO/DMU blends are shown in Fig. 6. When closely examined, several interesting features are observed in these thermograms. In all the blends, there is a well-defined PEO melting endotherm. Interestingly, peak minima for these endotherms (which is also taken as T_m values) show a small but gradual decrease to lower temperatures as the amount of PEO in the blend decreases. Blends containing 10 and 25 wt% DMU do not show well-defined high temperature melting endotherms. Other blends containing 50, 67, 75 and 90% DMU show fairly broad, unsymmetrical high temperature melting endotherms, which are all skewed towards lower temperatures. All these results clearly indicate extensive mixing between DMU and PEO, extent of which depends on the blend composition. It is also very interesting to note that a pure DMU phase is not present in any blend, clearly confirming the presence of very strong hydrogen bonding interaction between (N–H) groups in DMU and the ether (C–O–C) oxygen in PEO. Consecutive heating and cooling cycles applied to the blends do not have any effect on their DSC

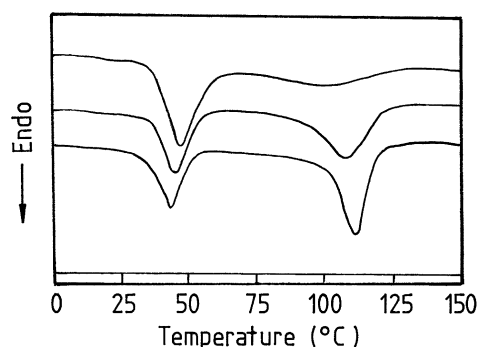


Fig. 7. DSC thermograms for PEO/URTN blends. From top to bottom: 75/25, 50/50, and 25/75 PEO/URTN by weight.

behavior, indicating that the morphologies formed were stable. Table 3 gives summary of the results on the melting behavior of PEO/DMU blends, which includes peak ranges, melting points and ΔH_{fus} values, obtained from the analyses of DSC endotherms.

DSC thermograms of PEO/URTN blends are shown in Fig. 7. These blends also display almost identical behavior to that of PEO/DMU blends. As the amount of PEO in the system increases, melting endotherm of the URTN becomes broader and shifts to lower temperatures. This behavior shows strong interaction and mixing between PEO and URTN, leading to the formation of a new crystalline structure. As observed in PEO/DMU blends, in these systems also, peak minima for PEO endotherms show gradual shift to lower temperatures as the amount of PEO decreases. However, the magnitude of the shift is smaller. Table 4 gives the summary of DSC results on the melting behavior of PEO/URTN blends.

Several important trends are observed from the analyses of DSC results on PEO/DMU and PEO/URTN blends. These are

1. All the blends consist of a pure PEO phase and a mixed, crystalline PEO/DMU or PEO/URTN phase. Pure DMU or pure URTN phases do not exist in any blend at any composition.
2. Blends containing less than 25 wt% DMU do not show a

Table 3
Summary of DSC results on melting behavior of PEO, DMU and PEO/DMU blends

Sample description	PEO endotherm			DMU endotherm		
	Peak range (°C)	T_m (°C)	ΔH_{fus} (J/g)	Peak range (°C)	T_m (°C)	ΔH_{fus} (J/g)
PEO	37–57	49	150.5	–	–	–
PEO/DMU (90/10)	20–52	47	134.2	–	–	–
PEO/DMU (75/25)	22–55	45	104.5	–	–	–
PEO/DMU (50/50)	20–48	43	72.7	60–102	89	29.3
PEO/DMU (33/67)	18–48	41	42.2	60–107	95	62.3
PEO/DMU (25/75)	16–46	38	25.9	65–109	102	84.9
PEO/DMU (10/90)	10–40	34	13.8	80–110	105	95.3
DMU	–	–	–	90–117	108	123.3

Table 4
Summary of DSC results on melting behavior of PEO, URTN and PEO/URTN blends

Sample description	PEO endotherm			URTN endotherm		
	Peak range (°C)	T_m (°C)	ΔH_{fus} (J/g)	Peak range (°C)	T_m (°C)	ΔH_{fus} (J/g)
PEO	37–57	49	150.5	–	–	–
PEO/URTN (80/20)	22–55	49	101.2	65–120	100	13.0
PEO/URTN (63/37)	20–48	48	75.6	75–120	105	27.6
PEO/URTN (50/50)	18–48	47	68.5	75–120	110	30.5
PEO/URTN (25/75)	16–46	46	39.7	90–123	114	52.3
URTN	–	–	–	110–135	120	79.0

well-defined high temperature melting endotherm in DSC.

- As the amount of PEO in the blend increases, high temperature endotherm shifts to lower temperatures and becomes much broader, indicating extensive mixing between PEO and DMU and URTN.
- Melting endotherm of pure PEO phase present in the blends shifts to lower temperatures as the amount of DMU or URTN in the blend increases.

These observations indicate extensive mixing between PEO and DMU and PEO and URTN due to strong hydrogen bonding interaction between ether oxygen in PEO and (N–H) in urea and urethane groups. This has also been predicted by QM calculations [18] and confirmed by IR results. As shown in Fig. 8, when T_m values of PEO/DMU and PEO/URTN blends are plotted against blend compositions, linear relationships are observed. This is an interesting observation, which clearly demonstrates that the extent of mixing is directly related to the blend composition.

3.3. Optical microscopy

DSC analyses of PEO/DMU and PEO/URTN blends indicated two-phase crystalline morphologies (a pure PEO phase and a mixed PEO/DMU or PEO/URTN phase, respectively) for these systems. In order to have a better understanding of the crystalline structures formed and their melting behavior, PEO/DMU blends were also investigated

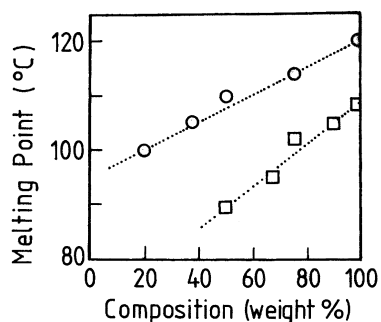
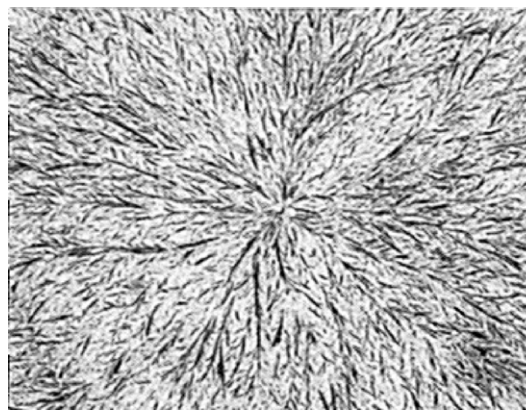


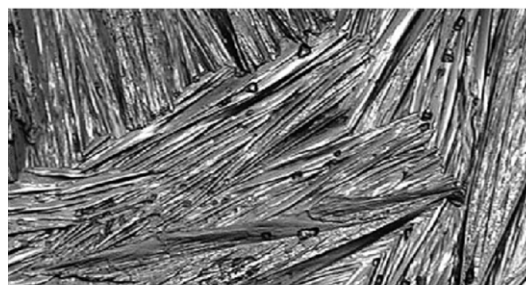
Fig. 8. Variation in the melting points of PEO/URTN (□) and PEO/DMU (○) blends with composition.

by hot stage optical microscopy. As discussed below, results obtained are very interesting and very supportive of the DSC behavior.

Fig. 9a and b show the OM pictures of crystalline morphologies of pure PEO and DMU obtained at 23 °C. Both of the materials display spherulitic structures. OM pictures obtained for two different magnifications of PEO/DMU 50/50 blend are displayed in Fig. 10a and b. As expected from DSC results, two separate crystalline phases are present in the blend; a pure PEO phase consisting of very well developed spherulitic crystals embedded between narrow, fibrillar type crystalline channels. These fibrillar crystalline structures, which are due to the complex formed between PEO and DMU, are very different from the structure of pure DMU (Fig. 9b). Formation of complex

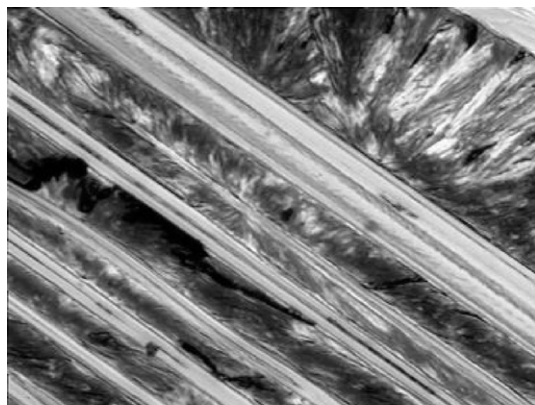


(a)

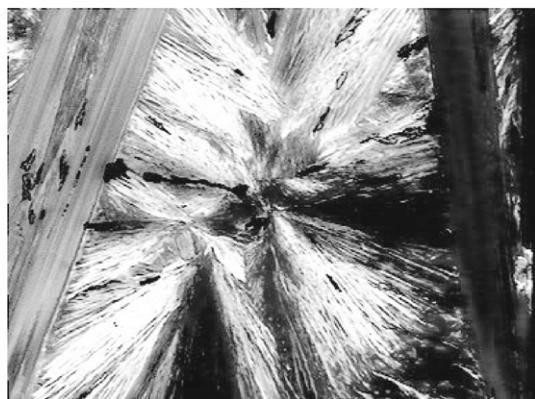


(b)

Fig. 9. Optical microscope pictures showing the crystalline morphologies of (a) PEO (5 ×) and (b) DMU (10 ×) at 23 °C.



(a)



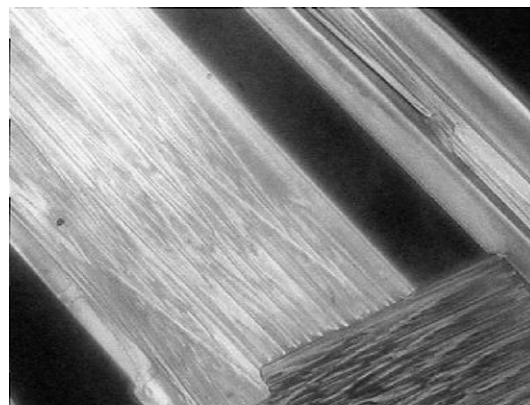
(b)

Fig. 10. Optical microscope pictures showing the crystalline morphology of 50/50 by weight PEO/DMU blend at 23 °C. (a) 10 × and (b) 50 ×.

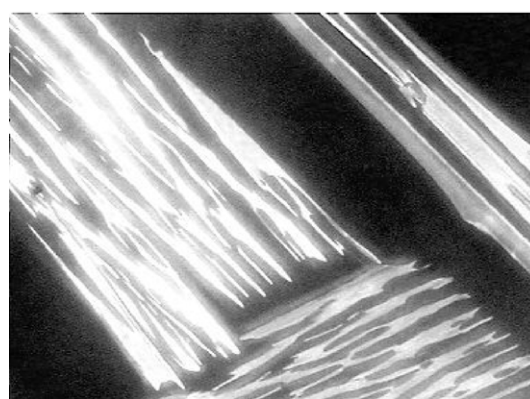
structures between PEO and urea and thiourea have also been reported [30,31]. Fig. 11a gives the structure of the PEO/DMU 50/50 blend heated to 50 °C, just above the melting point of PEO, which only shows the fibrillar structure of the mixed PEO/DMU phase. As the system is further heated to 75 °C, (Fig. 11b) this mixed phase starts melting slowly, which strongly support the observations made in DSC. As clearly shown in Fig. 6 and summarized on Table 3, high temperature melting endotherm of PEO/DMU 50/50 blend starts at 60 °C and extends all the way to 102 °C. From DSC results, at 75 °C, only a partial melting is expected, which is exactly the same as the behavior observed under microscope. When the molten blend is cooled to room temperature, the two-phase morphology shown in Fig. 10 is reproduced.

4. Conclusions

Influence of hydrogen bonding on the crystallization behavior, morphology, thermal properties and spectroscopic behavior of model ether/urethane (PEO/URTN) and ether/urea (PEO/DMU) blends has been investigated over a very



(a)



(b)

Fig. 11. Optical microscope pictures (50 ×) showing the morphology of 50/50 PEO/DMU blend at (a) 50 °C and (b) at 75 °C.

broad composition range. Under optical microscope, PEO/DMU blends show two different crystalline structures; a pure PEO phase and a mixed PEO/DMU phase. Interestingly a pure DMU phase is not present in these blends. These observations are strongly supported by FTIR and DSC findings. These results clearly indicate the presence of extensive hydrogen bonding between urea hydrogens in DMU and ether oxygen in PEO, which seems to completely destroy (N–H···C=O) type intermolecular hydrogen bonding between DMU molecules. When extended to microphase separated segmented polyurethane or polyurethaneurea copolymers, these observations suggest that crystalline urethane or urea hard domains are not pure, but always mixed with the soft polyether segments. A manuscript, showing the results on the nature and purity of hard segment domains in segmented polyurethane copolymers is in preparation.

References

- [1] Lelah MD, Cooper SL. Polyurethanes in medicine. Boca Raton, FL: CRC Press; 1986.
- [2] Oertel G. Polyurethanes handbook. Munich: Hanser Publishers; 1994.

- [3] Woods G. The ICI polyurethanes book. New York: Wiley; 1990.
- [4] Hepburn C. Polyurethane elastomers. Essex: Elsevier; 1992.
- [5] Bonart R, Muller EH. *J Macromol Sci Phys* 1974;B10:177.
- [6] Abouzahr S, Wilkes GL, Ophir Z. *Polymer* 1982;23:1077.
- [7] Koberstein JT, Galambos AF, Leung LM. *Macromolecules* 1992; 25(23):6195–204.
- [8] Cooper SL, Tobolsky AV. *J Appl Polym Sci* 1966;10:1837–44.
- [9] Lee HS, Wang YK, Hsu LS. *Macromolecules* 1987;20(9):2089–95.
- [10] Brunette CM, Hsu SL, MacKnight WJ. *Macromolecules* 1982;15(1): 2215–21.
- [11] Huh SD, Cooper SL. *Polym Engng Sci* 1971;11:369.
- [12] Ning L, De-Ning W, Sheng-Kang Y. *Macromolecules* 1997;30: 4405–9.
- [13] Garrett JT, Runt J, Lin JS. *Macromolecules* 2000;33(17):6353–9.
- [14] Yilgor E, Burgaz E, Yurtsever E, Yilgor I. *Polymer* 2000;41(3): 849–57.
- [15] Yilgor E, Tulpar A, Kara S, Yilgor I. Silicones and silicone modified materials. In: Clarson SJ, Fitzgerald JJ, Owen MJ, Smith SD, editors. ACS symposium series, vol. 729. Washington, DC: ACS; 2000. Chapter 26.
- [16] Yilgor E, Yilgor I. *Polymer* 2001;42(19):7953–9.
- [17] Coleman MM, Painter PC. *Prog Polym Sci* 1995;20:1–59.
- [18] Yilgor E, Yilgor I, Yurtsever E. *Polymer* 2002; in press.
- [19] Coleman MM, Skrovanek DJ, Hu J, Painter PC. *Macromolecules* 1988;21(1):59–66.
- [20] Chamberlin Y, Pascault JP. *J Polym Sci Polym Chem* 1983;21:415.
- [21] McClusky JW, Pocol M, Alvarez N. *Polym Prepr* 1999;39(2):661–2.
- [22] Ning L, De-Ning W, Sheng-Kang Y. *Polymer* 1996;37(16):3577–83.
- [23] Saiani A, Daunch WA, Verbeke H, Leenslang JV, Higgins JS. *Macromolecules* 2001;34(26):9059–68.
- [24] Noshay A, McGrath JE. Block copolymers: overview and critical survey. New York: Academic Press; 1977.
- [25] Teo LS, Chen CY, Kuo JF. *Macromolecules* 1997;30(6):1793–9.
- [26] Fernandez AM, Lozano AE, Gonzales L, Rodriguez A. *Macromolecules* 1997;30(12):3584–92.
- [27] Yen FS, Hong JL. *Macromolecules* 1997;30(25):7927–38.
- [28] CRC handbook of chemistry and physics. 78th ed. Boca Raton: CRC Press; 1997. p. 3–328.
- [29] Bailey Jr FE, Koleske JV. Poly(ethylene oxide). New York: Academic Press; 1976.
- [30] Parrod J, Kohler A, Hild G, Mayer R. *J Polym Sci, Part C* 1968;16: 4063.
- [31] Tadakaro H. In: Peterlin A, Goodman M, Okamura S, Zimm BH, Mark HF, editors. *Macromolecular reviews*. New York: Interscience Publishers; 1967. p. 119.